

Development of a Wind Turbine LiDAR Simulator

David Schlipf, Juan José Trujillo, Valeria Basterra and Martin Kühn
Endowed Chair of Wind Energy (SWE), Universität Stuttgart
Allmandring 5B, 70569 Stuttgart, Germany
+49(0)711/685 68254, david.schlipf@ifb.uni-stuttgart.de

Abstract

Remote sensing techniques like LiDAR offer many novel applications to the wind energy community, e.g. fast and accurate measurements of inflow and wake wind fields from the turbine nacelle. The prospects of such a new technique are evaluated with a software tool simulating a nacelle-based LiDAR system. The paper presents the implementation and application of a simulator that has been conceived to support the design of wind field scanning procedures. The tool helps to optimize the hardware setup, scanning trajectories and frequency. Furthermore it can be coupled with an aeroelastic code with the aim of developing a predictive control based on remote sensing.

1 Introduction

In the framework of the German joint project "Development of LiDAR measurement techniques for the German offshore test site" new LiDAR techniques are tested and developed to support the deployment and operation of large wind turbines, especially offshore. One topic within this project is the test of a LiDAR system mounted on wind turbine nacelles with two main objectives. Namely, the fast and accurate measurement of inflow and wake wind fields, and the evaluation of the use of inflow measurements for improved wind turbine control.

In this paper the development of a simulation tool is shown which reproduces the operation of a nacelle-mounted LiDAR system in a realistic way. After the explanation of the purpose of the LiDAR simulator in Chapter 2, the implementation of the modularized simulator is described in Chapter 3. The five main components are illustrated, namely the scanning of a synthetic wind field, the simulation of the measurement, blade collision detection, correction of the direction and finally the interpolation. Two applications of the simulator are presented in the following sections. In Chapter 4 the design of a new scanning system for adaptation of a standard

ground-based LiDAR system for nacelle-based measurements on a 5MW wind turbine (see Figure 1) is investigated. Different scanning strategies for inflow and wake measurements are evaluated in terms of their accuracy. Recommendations about the best-suited scanning hardware, trajectories and frequency are derived [1]. In Chapter 5 the coupling of the simulator with an aeroelastic code through Simulink is addressed to evaluate predictive control strategies based on near-inflow measurements [2]. First experiences with this coupling are presented. Conclusions and further research can be found in Chapter 6.



Figure 1: Sketch of a LiDAR system mounted on the nacelle of the MULTIBRID M5000

2 The Purpose of a LiDAR Simulator

The main objective is the development of a simulation tool which reproduces the operation of a nacelle-mounted LiDAR system with the following characteristics: The tool facilitates the evaluation of scanning patterns to find the best hardware and software solution for applications like control, power curve assessment and wake measurements. An interface with Simulink has been implemented to test wind turbine control strategies based on LiDAR. A modular setup provides software parts that can be used to process measurement data in the same way as simulated data.

3 The modular Implementation

The code for the **Wind Turbine LiDAR Simulator (WITLIS)** is realized in Matlab with a modularized philosophy with the aim of great flexibility. The simulator reads in synthetic wind fields generated with an external program such as TurbSim or WindSim. The following five sections describe the main components of the simulator.

3.1 Scanning of a synthetic wind field

To simulate the scanning procedure, the focus point positions $[t_{fp}, x_{fp}, y_{fp}, z_{fp}]$ in time and space with respect to hub position are calculated depending on the selected periodic or non periodic trajectory, sampling frequency and scanning range. Hardware restrictions of the scanner such as speed or angle limitations as well as different hardware architectures can be considered. As shown in [1], scanners with rotating parts like Risley prisms favor periodic Lissajous figures (Figure 2) while devices with moving mirrors qualify for TV-scans (Figure 3).

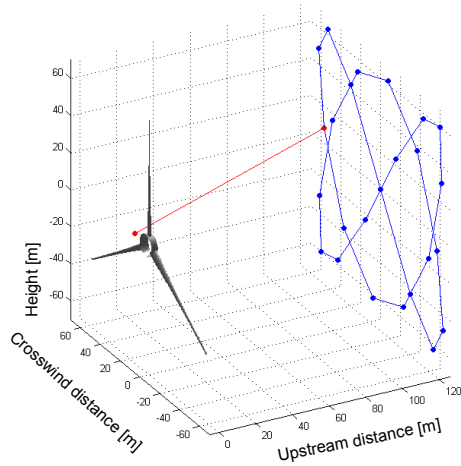


Figure 2: Lissajous scanning trajectory

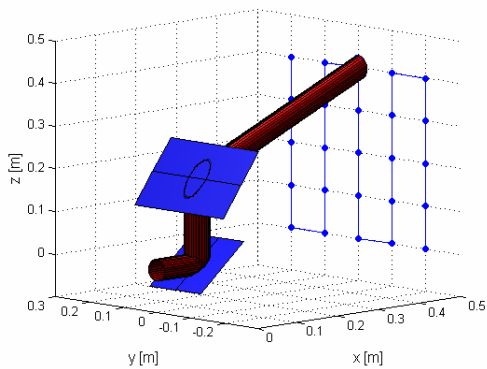


Figure 3: TV scan (scaled) with two one-degree-of-freedom-mirrors

Due to the modular code design further scanning strategies can be analyzed. These include fixed focus points realized e.g. with different fixed LiDAR sources or beam splitter as well as the possibility of pulsed LiDAR systems to scan at different distances at the same time.

3.2 Simulation of the measurement

A three dimensional turbulent wind field as commonly used for aeroelastic load analysis is calculated in advance. One measurement of a line-of-sight wind velocity v_{los} is simulated by a spatial and temporal interpolation of the wind field in different points distributed in the sample volume of a laser beam.

Given the static position \mathbf{P}_{LiDAR} of the LiDAR system, the direction vector of the laser beam \mathbf{a}_l and the components of the normalized vector write as follows:

$$\mathbf{a}_l = \begin{bmatrix} x_{fp} \\ y_{fp} \\ z_{fp} \end{bmatrix} - \mathbf{P}_{LiDAR}, \quad \begin{bmatrix} x_l \\ y_l \\ z_l \end{bmatrix} = \frac{\mathbf{a}_l}{|\mathbf{a}_l|} \quad (1)$$

Assuming Taylor's frozen turbulence hypothesis, the time, crosswind distance and height of the different points of the laser beam in the wind field grid are calculated by

$$\mathbf{P}_{fp}(r) = \begin{bmatrix} t_{fp} + \frac{x_{fp} + rx_l}{v_{mean}} \\ y_{fp} + ry_l \\ z_{fp} + rz_l \end{bmatrix}, \quad r \in \left[-\frac{l}{2}, \frac{l}{2}\right] \quad (2)$$

where v_{mean} is the mean longitudinal wind speed of the wind field, l the pulse length and r the distance to the focus point.

In Figure 4 different energy distributions depending on the pulse length and LiDAR type (pulsed/continuous wave) are shown [3].

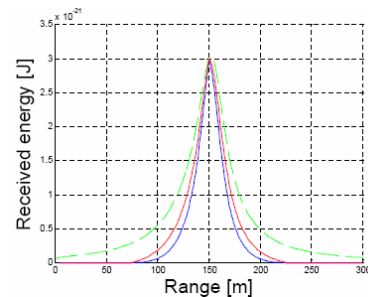


Figure 4: Confinement profiles for a pulsed and continuous wave LiDAR [3]

These distributions are used to derive different weighting functions $f(r)$ with respect to the distance r from the focus point. The wind field

components u , v , w in $\mathbf{P}_{fp}(r)$ are obtained by interpolation. Finally the line-of-sight velocity is calculated:

$$v_{los} = \int_{-\frac{l}{2}}^{\frac{l}{2}} (x_l u(r) + y_l v(r) + z_l w(r)) f(r) dr \quad (3)$$

3.3 Collision detection

The simulator can be coupled to a simple wind turbine model with variable rotor speed or a more complex, aeroelastic one which consider elastic deformations of the wind turbine structure (see Chapter 5). Depending on rotor blades and LiDAR position, collisions with the laser beam are detected and associated focus points are ignored.

3.4 Correction of the direction

In the sections above it is described how the simulated measurements are obtained. The following two sections present methods that retrieve wind fields from the simulated and further on from real measurements.

With one LiDAR system only the projection of a wind vector in beam direction can be measured. For retrieving a 3D vector, the missing two dimensions can be replaced by two assumptions, e.g. the horizontal and vertical components of the wind vector are zero, assuming that the wind turbine is aligned with the mean wind direction. The correction to \mathbf{a}_{cor} depending on the original wind vector \mathbf{a}_{wnd} is depicted for two situations in Figure 5.

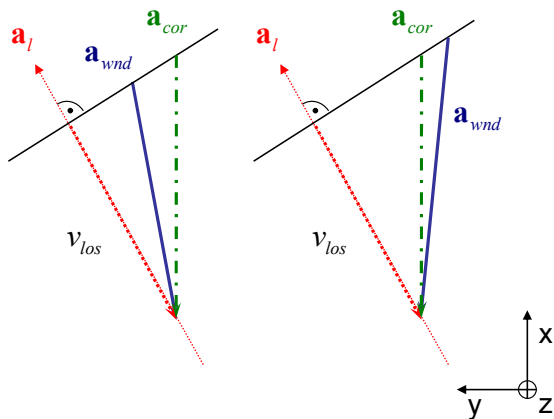


Figure 5: 2D view of the direction correction assuming crosswind direction is zero

It can be seen that the correction will lead to both over- and underestimations of the actual local wind speed which is considered to be more appropriated then the systematic

underestimation that would occur if the line-of-sight wind speed would be taken directly.

3.5 Interpolation

Depending on the application, the simulated measurements are interpolated to adequate grids. The process is performed by means of a linear interpolation with a Delaunay triangulation of the scanned area based on the simulated points. For post-processing purposes the different wind components (u , v , w) in a wind field grid (time, crosswind distance and height) are computed with a 3D interpolation. As normally the vertical component v and the horizontal component w are assumed to be zero (Section 3.4), the interpolation is just done for the inflow wind component u . This module can also be used for data processing with real measurements. For online applications like LiDAR control (Section 5) a 2D interpolation is employed, if there was a scanning only in one distance, in order to avoid extrapolation in time. A group of points, e.g. the last points forming a closed scan trajectory, are interpolated only in space (crosswind distance and height) and assigned to the time of the last point (Figure 6).

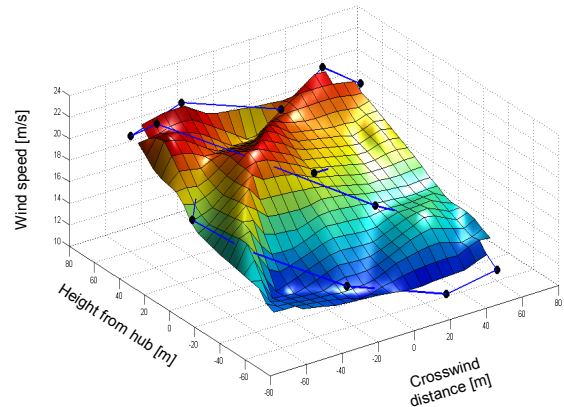


Figure 6: Interpolation of scanned inflow wind speed (Example snapshot 2 s)

The interpolated and the synthetic wind field can be compared to evaluate the accuracy of the simulated measurements. The effects of the different steps such as collision, volume measurement, assumptions and interpolation can be estimated and used to optimize the procedure.

4 Optimization of scanning hardware and software

The simulation tool described above supports the design of a new scanning system for the adaptation of a standard ground-based LiDAR system for nacelle-based measurements. Figure 7 shows the iterative procedures: Different applications such as control, wake model verification or power curve assessment require different spatial and temporal resolutions of the measured wind field. With WITLIS scanning strategies are designed and evaluated in their accuracy. Recommendations for the scanning hardware are given. The scanning device restrictions such as velocity constraints of moving scanner parts require a redesign of the scanning strategy. On the other hand, wind fields from simulated or real measurements are used for testing the applications and requirements description is improved.

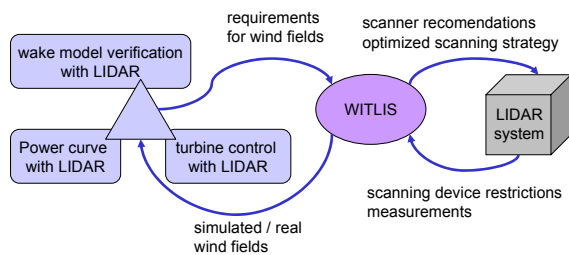


Figure 7: Interactions between the applications, the simulator and the LiDAR system

In a first study [1] the Lissajous figure with a frequency ratio of 2:3 and a phase difference of $\pi/2$ (see Figure 2) turns out to be the best choice with respect to other trajectories, when one is interested in a scan of the entire wind field. Figure 8 shows a snap shoot of the interpolated inflow wind speed scanning a synthetic wind field with $v_{mean} = 16$ m/s, turbulence intensity $TI = 18\%$ and time resolution of 0.25 s. Figure 9 shows a snap shoot of the synthetic inflow wind speed at the same time. One measurement is taken every 0.05 s and 25 points per trajectory, a simplified weighting function for a pulsed LiDAR system with measuring volume of 20 m is used, measurement with blade collision of a simplified 5MW turbine are ignored and the inflow wind speed is retrieved from line-of-sight speed assuming horizontal and vertical wind speed are zero.

The correlation between Figure 8 and Figure 9 has to be compared to the requirements for the wind fields. To find the best solution for each application and the specific hardware, further research has to be undertaken regarding

LiDAR control and wake measurements to redefine optimization criteria.

The recommendation of this first study served for the design of the scanning hardware. The complexity of this optimization problem demands the scanner to be as flexible as possible to test other trajectories.

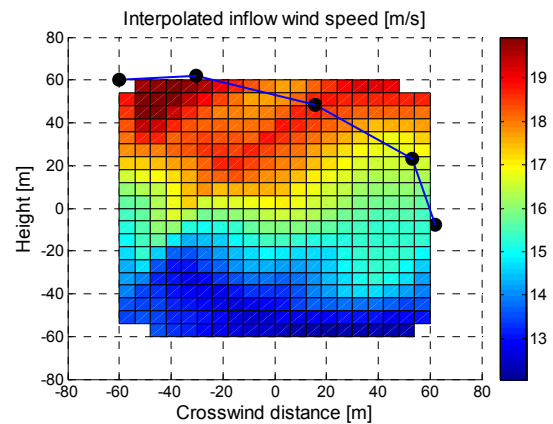


Figure 8: interpolated inflow wind speed

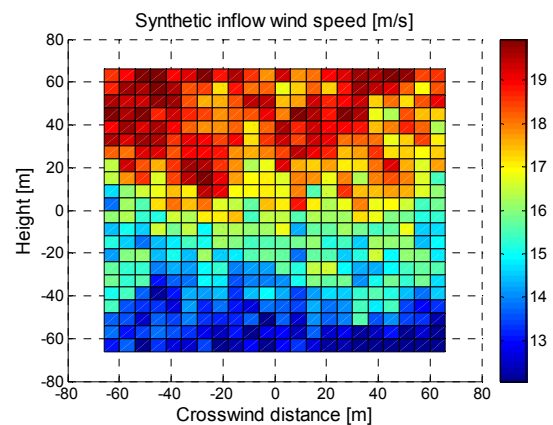


Figure 9: synthetic inflow wind speed at the same time as Figure 8

5 Testing of LiDAR Control

The Predictive Disturbance Compensation (PDC) based on near-inflow measurements in front of a turbine is a promising control strategy to reduce fatigue and extreme loads on turbines. So far [2] knowledge of the full future wind field is assumed. Through coupling WITLIS with the Simulink/Fast implementation of the controller a more realistic setup is simulated.

Figure 10 presents the simulation arrangement: A TurbSim wind field (TS) is scanned online with the Lissajous scanning trajectory proposed above at a distance of one rotor diameter in front of the turbine, simulating a LiDAR System.

The same wind field serves as input for the wind turbine (WT) modeled in FAST. The interpolated wind field (LS) is passed to the controller (PDC) in every time step. With this information the feed forward controller tries to compensate for wind field fluctuations like gusts.

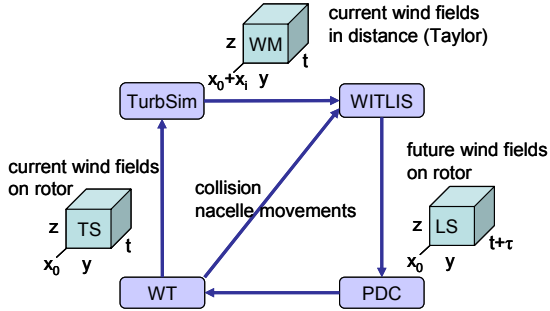


Figure 10: Flowchart of the LiDAR control testing simulation

For the Predictive Disturbance Compensation the impact on the wind field has to be predicted. Therefore the 3D wind field is reduced to an effective wind speed through a weighting of the inflow wind speed. It is assumed that wind fields with the same effective wind speed cause the same impact on the wind turbine [2].

Contrary to [2] the following errors in the effective wind speed are taken into account:

- *Finite measurements*
According to the selected scanning trajectory, the wind field is scanned only in finite points in every time step.
- *Volume measurement*
As LiDAR systems always measure a probe volume (Section 3.2), the wind speed is not exactly scanned.
- *Wind turbine interferences*
The controlled wind turbine interferes with the LiDAR system changing the absolute position through nacelle movements and through collision of the blades with the laser beam.

Figure 11 compares the more realistic setup of a LiDAR controlled turbine (dotted) with the perfect setup (solid) from [2] and a conventionally PI controlled turbine (dashed).

From Figure 11 and Table 1 it can be seen that still with this more realistic setup, the PDC results to a better regulation of the rotor speed. This leads to a reduction of the fore-aft bending moment at the tower base M_{yT} without higher pitch dynamics.

Table 1: Standard deviation of the signals from Figure 11

	PI	PDC	PDC _w	PDC _w /PI
$\sigma(\Omega)$ [MNm]	0.48	0.10	0.17	35%
$\sigma(M_{yT})$ [MNm]	15.1	9.8	11.8	78%
$\sigma(d\beta/dt)$ [deg/s]	0.79	0.53	0.65	83%

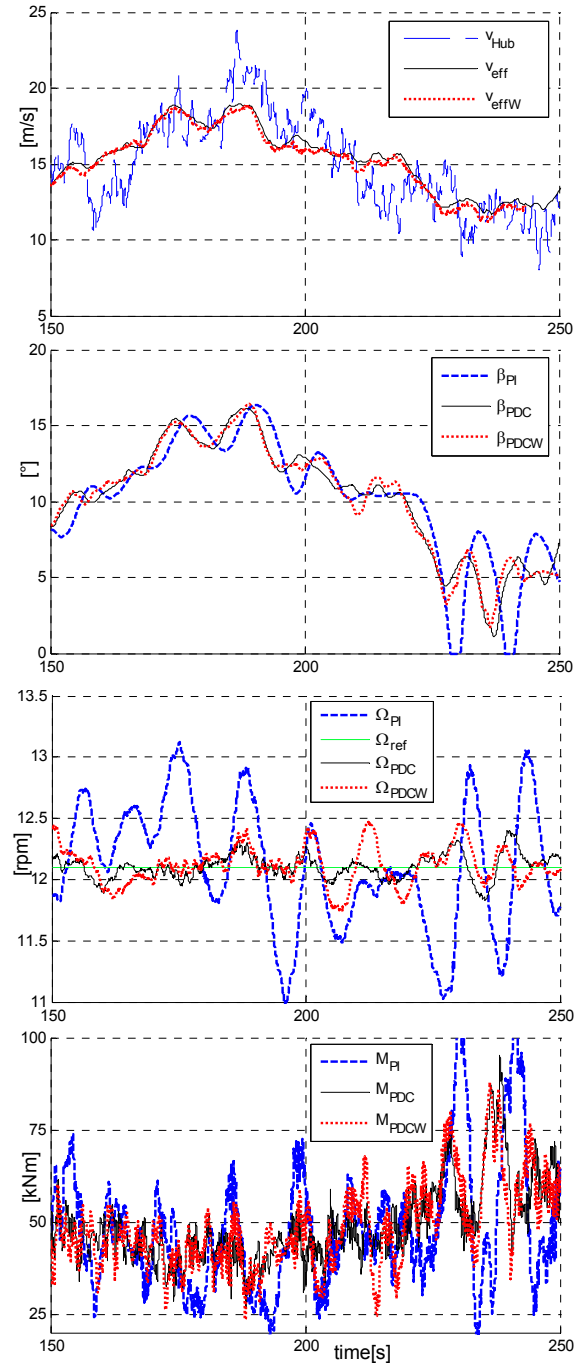


Figure 11: Turbulence inflow with effective wind speed, reaction pitch angle, fore-aft bending moment and rotor speed for the different setups

6 Conclusions and Outlook

In order to support the design and testing of nacelle-based LiDAR applications a simulation tool has been developed. The software WITLIS (Wind Turbine LiDAR Simulator) realistically reproduces the LiDAR system operating under turbulent wind inflow and its interaction with the wind turbine.

With the present implementation the first step of an optimization of scanning hardware and software has been realized as well as an evaluation of the performance of predictive control strategies based on more realistic near-inflow measurements.

Further research will focus on the redesign of the presented scanning strategies for the different applications as well as for the specific scanner hardware which is currently developed within the above mentioned project. PDC is planned to be applied to cyclic or individual pitch.

Acknowledgements

This research is undertaken in the framework of the German joint research project "Development of LiDAR measurement techniques for the German offshore test site" (0327642) funded by The German Federal Ministry for the Environment, Nature Conservation and Nuclear Safety.

References

- [1] V. Basterra, *Evaluation of Scanning Strategies of a Nacelle Mounted LiDAR System for Inflow and Wake Measurements on a Wind Turbine*, Master Thesis, Universidad Pontificia Comillas, Madrid, Spain, 2008.
- [2] D. Schlipf, M. Kühn, *Prospects of a Collective Pitch Control by Means of Predictive Disturbance Compensation Assisted by Wind Speed Measurements*, DEWEK 2008, Bremen, Germany, 2008.
- [3] P. Lindelöw, *Fiber Based Coherent Lidars for Remote Wind Sensing* Ph.D. thesis, Danish Technical University, Copenhagen, Denmark, 2008.